Published in final edited form as:
*J Mol Cell Cardiol*. 2014 November ; 0: 159–168. doi:10.1016/j.yjmcc.2014.08.021.

# Connexin40 abnormalities and atrial fibrillation in the human heart

**Joanna Gemel**[1], **Andrew E. Levy**[1], **Adria R. Simon**[1,*], **Katherine B. Bennett**[1], **Xun Ai**[2], **Shahab Akhter**[3], and **Eric C. Beyer**[1]

[1]Department of Pediatrics, University of Chicago, Chicago, IL, USA

[2]Department of Pharmacology, Loyola University School of Medicine, Maywood, IL, USA

[3]Department of Surgery, University of Wisconsin, Madison, WI, USA

## Abstract

Normal atrial conduction requires similar abundances and homogeneous/overlapping distributions of two connexins (Cx40 and Cx43). The remodeling of myocyte connections and altered electrical conduction associated with atrial fibrillation (AF) likely involves perturbations of these connexins. We conducted a comprehensive series of experiments to examine the abundances and distributions of Cx40 and Cx43 in the atria of AF patients. Atrial appendage tissues were obtained from patients with lone AF (paroxysmal or chronic) or normal controls. Connexins were localized by double label immunofluorescence confocal microscopy, and their overlap was quantified. Connexin proteins and mRNAs were quantified by immunoblotting and qRT-PCR. PCR amplified genomic DNA was sequenced to screen for connexin gene mutations or polymorphisms. Immunoblotting showed reductions of Cx40 protein *(to 77% or 49% of control values in samples from patients with paroxysmal and chronic AF, respectively)*, but no significant changes of Cx43 protein levels in samples from AF patients. The extent of Cx43 immunostaining and its distribution relative to N-cadherin were preserved in the AF patient samples. Although there was variability of Cx40 staining among paroxysmal AF patients, all had some fields with substantial Cx40 heterogeneity and reduced overlap with Cx43. Cx40 immunostaining was severely reduced in all chronic AF patients. qRT-PCR showed no change in Cx43 mRNA levels, but reductions in total Cx40 mRNA *(to <50%)* and Cx40 transcripts A *(to ~50%)* and B *(to <25%)* as compared to controls. No Cx40 coding region mutations were identified. The frequency of promoter polymorphisms did not differ between AF patient samples and controls. Our data suggest that reduced Cx40 levels and heterogeneity of its distribution (relative to Cx43) are common in AF. Multiple mechanisms likely



✉Address correspondence to: Eric C. Beyer, M.D., Ph.D., Professor of Pediatrics, University of Chicago, 900 E. 57th St. KCBD 5152, Chicago, IL 60637, Tel: 773-834-1498, FAX: 773-834-1329, ecbeyer@uchicago.edu.
*Present address, School of Medicine, New York University, New York, NY 10016

**Disclosures:**
Conflicts of interest: none for any of the authors

lead to reductions of functional Cx40 in atrial gap junctions and contribute to the pathogenesis of AF in different patients.

**Keywords**

atrial fibrillation; gap junction; connexin; arrhythmia; Connexin40

## 1. Introduction

Atrial fibrillation (AF) is the most common cardiac arrhythmia. It is characterized by a rapid and irregular electrical activation and the loss of atrial muscle contractility. The pathogenesis of AF involves initiating triggers (often rapidly firing ectopic foci located inside the pulmonary veins) and an abnormal atrial tissue substrate that maintains the arrhythmia [1, 2]. The tissue substrate is determined in large part by the abundance and distribution of intercellular channels contained within atrial gap junctions [3]. Gap junction channels allow the exchange of ions (and small molecules) between adjacent cells. These channels are critical for normal electrical conduction in all regions of the heart.

Atrial gap junctions are comprised of two different subunit proteins, Connexin40 (Cx40) and Connexin43 (Cx43). They are each abundantly expressed by atrial myocytes with similar abundances and highly overlapping distributions. Together, Cx40 and Cx43 determine the properties of intercellular conduction within this tissue [4, 5]. Various alterations of both Cx40 and Cx43 have been observed in animals and human patients with AF (reviewed in [6]). *However, these studies have produced confounding results that may have resulted from the different etiologies and durations of AF in these patients, the extent of failure, and structural heart disease. Some previous investigations only examined individual aspects of connexin biology, like distribution, expression, mutations, or gene polymorphisms.*

*Therefore, we sought to perform a comprehensive study of human AF patients (and controls) covering as many aspects of connexin expression and distribution as can be studied with currently available tools. We also sought to avoid confounding issues that might arise due to pre-existing valvular disease or myocardial failure.* About 15% of AF patients have “lone AF” which develops in apparently normal hearts in the absence of structural abnormalities. We studied the atrial tissue obtained from a group of patients who underwent surgical ablation of their lone AF. The differences in distributions and abundances of Cx40 and Cx43 were evaluated as were possible genetic reasons for those abnormalities.

## 2. Materials and Methods

### 2.1. Patients and tissues

Tissue samples from the left atrial appendage were obtained during surgical ablation of the arrhythmia in patients with atrial fibrillation (by SA). Immediately after collection, tissue samples were snap frozen in liquid nitrogen and stored at −80 °C. This protocol was approved by the Institutional Review Boards at the authors’ institutions.

All patients had lone AF, without evidence of structural heart disease or abnormal heart function. Although patient samples were de-identified, limited patient information is summarized in Supplemental Table 1. The study included 8 patients with chronic AF (CAF) and 16 patients with paroxysmal AF (PAF). 8 control samples were obtained from hearts not used for transplantation. All groups contained both females and males. The patients were predominantly Caucasian (one African American). The ages of patients ranged from 26 to 85 with an average age of 52 across all groups.

The quality of all samples was judged to be excellent based on our abilities to isolate protein and intact nucleic acids and to perform histology. However, for some samples, the limited amounts of tissue precluded performing all assays (like quantitative confocal microscopy). All CAF (8) and PAF (16) samples were used for immunoblots and qRT-PCR.

### 2.2. Antibodies and fluorescent lectin

Cx40 was detected using rabbit polyclonal antibodies directed against the carboxy-terminal domain of Cx40 (cat. no 36-4900 Life Technologies, Grand Island, NY). It was used at 1:300 dilution for immunofluorescence and at 1:1000 dilution for immunoblotting. Cx43 was detected using a mouse monoclonal antibody directed against amino acids 252-270 (MAB 3067, Millipore/Chemicon, Billerica, MA) for immunofluorescence at dilution 1:200 or using rabbit polyclonal antibodies directed against amino acids 363-382 of human/rat Cx43 (C6219, SIGMA Chemical Company, St. Louis, MO) at 1:1000 dilution for immunofluorescence and at 1:10,000 dilution for immunoblotting. Mouse monoclonal anti-N-cadherin antibodies (cat. no 33-3900 Life Technologies, Grand Island, NY) were used at 1:500 dilution for immunofluorescence. Mouse monoclonal anti-GAPDH antibodies were obtained from Life Technologies (cat. no 39-8600) and used at 1: 500 dilution for immunoblotting to verify accuracy of protein loading after treating blots with Restore Plus Western blot stripping buffer (Thermo Fisher Scientific Inc., Waltham, MA). Cy3-conjugated goat anti-rabbit IgG and HRP-conjugated goat anti-rabbit or anti-mouse IgG antibodies were obtained from Jackson ImmunoResearch (West Grove, PA).

Wheat Germ Agglutinin (WGA)-Texas Red®-X conjugate (Life Technologies) was used at 1:200 dilution.

### 2.3. Immunoblot analysis

Heart tissue was disrupted in a glass Kontes homogenizer using 25–100 μl of 50 mM Tris-HCl (pH 8.0) buffer containing 150 mM NaCl, 1% Triton X-100, 0.02% sodium azide, 50 mM sodium fluoride, 0.5 mM sodium orthovanadate, and Roche mini EDTA-free protease inhibitors (Roche Applied Science, Indianapolis, IN) (one tablet per 5 ml of lysis buffer)[5].

The protein concentrations of homogenates were determined using the method of Bradford (1976) [7] (Bio-Rad, Richmond, CA). Aliquots containing 2.5 μg of protein were separated by SDS-PAGE on 10% polyacrylamide gels and blotted onto Immobilon-P membranes (Millipore, Bedford, MA). [5] Rainbow molecular weight marker standards (GE Healthcare Biosciences, Pittsburgh, PA) were used to calibrate the gels. Immunoblots were developed with ECL chemiluminiscence reagents (GE Healthcare Biosciences) and exposure to X-ray film.

### 2.4. Immunohistochemistry

Four to six cryosections (approximately 8 μm thick) of each left atrial appendage sample were put on one slide. At least four slides were prepared for each patient sample. Slides were fixed with 3% paraformaldehyde for 15 minutes and then blocked for 30 minutes at room temperature using buffer composed of 10% heat inactivated normal goat serum in PBS containing 0.75% Triton X-100. Slides were then incubated with primary antibodies diluted in blocking solution overnight at 4 °C. Following incubation with primary antibodies, slides were washed six times for five-minutes with PBS. Each slide was then incubated with secondary reagents at room temperature for 75 minutes. *For WGA staining, the blocking step was omitted; fixed sections were incubated for 10 min with WGA-Texas Red-X*. Afterwards, the slides were extensively rinsed again with PBS. Each slide was mounted with a cover slip using Prolong Gold anti-fade reagent (Life Technologies). Slides were sealed and stored in darkness at 4 °C.

### 2.5. Confocal imaging

A Leica TCS SP2 laser scanning confocal microscope was used to examine the distributions and co-localization of Cx40 and Cx43 or a connexin and N-cadherin in human atrial sections. For each patient, at least five images were captured using the 63X glycerol immersion objective. For co-localization studies each image included 3 channels: Cy3, Cy2, and differential interference contrast (DIC). Snapshots of images from each channel as well as all combinations of channel overlap were recorded. For all samples, the laser voltage at which images were captured in each filter was kept constant in order to minimize differences in connexin detection between samples. Images were acquired using sequential laser scanning to avoid bleed-through. The plane and quality of sections were evaluated using DIC, and flat, even sections were subsequently photographed. All images were captured within one week of sectioning and staining. *Images of sections stained with WGA-Texas Red-X were captured using a 20X objective (at least 5 images per sample).*

### 2.6. Analysis of confocal images

**2.6.1. Colocalization analysis—**Image analysis for colocalization of Cx43 and Cx40 (or connexins and N-cadherin) was performed using the JACoP plugin for Image J software (http://rsb.info.nih.gov/ij/) as described by Bolte and Cordelières, 2006. [8] The program analyzes image pairs of the same visual field using a compilation of general colocalization indicators. In the present study, each image pair consisted of one image from the Cy3 channel for Cx40 and one image from the Cy2 channel for Cx43. All images were acquired in such a way as to minimize variation in connexin staining intensity within each channel. Image pairs were analyzed using Mander's coefficients, which do not use average pixel intensity in evaluating colocalization. Mander's coefficients' are, however, very sensitive to non-specific staining or "background." In order to exclude such non-junctional staining from the Mander's calculation, a threshold level of pixel intensity was measured and subtracted from each image. We determined the areas encompassed by gap junction staining (for each connexin) based on the number of pixels above threshold intensity using Image J [8] similarly to the approaches described previously [9, 10]. The extent of overlap of the two connexins in each double label pair was quantified using the Colocalization Threshold plug-

in to the Image J software. A single Mander's calculation produces two colocalization coefficients, M1 and M2, with values between 0 (no colocalization) and 1 (perfect colocalization). In this paper, M1 is an expression of the overlap of Cx43 on Cx40 (Cx40 pixels that also contain Cx43), while M2 is a measure of the overlap of Cx40 on Cx43 (Cx43 pixels that also contain Cx40).

**2.6.2. Extracellular space assessment using WGA staining—**WGA is a lectin that binds to glycoconjugates and has been used to assess the abundance and distribution of cell membranes and the extracellular matrix in cardiac tissues [11, 12]. In normal and hypertrophic hearts, the distribution of WGA staining is similar to that of Masson's trichrome, which is commonly used to detect collagen/fibrosis [12]. Tissue staining with fluorescent WGA was analyzed using Image J software (http://rsb.info.nih.gov/ij/). The area of fluorescence (WGA-reactive tissue) was determined after conversion to binary (black and white) images by applying the automatic threshold level of pixel intensity. Tissue area was calculated by subtracting areas not covered with tissue ("holes") from the whole image area. The threshold for quantification of "hole area" was determined by side-by-side comparison of the binary and original color images, and the same threshold was used for all images. The percentage of WGA-reactive atrial tissue was calculated by dividing fluorescent image area by total tissue area.

### 2.7. Isolation of RNA and quantification of connexin mRNA levels

RNA was isolated from left atrial appendage samples (33–66 mg) using the miRNeasy Mini Kit (Qiagen, Germantown, MD). The quality of RNA was assessed using an Agilent 2100 Bioanalyzer (Agilent Technologies, Inc., Santa Clara, CA). All samples had RNA Integrity Number (RIN) values in the excellent quality range (7.7 – 9.6).

Levels of Cx40 and Cx43 mRNAs were quantified using real time qRT-PCR using a similar approach to that which we previously used to quantify Cx40 and Cx43 in in mouse myocyte samples [5]. cDNA was prepared from total RNA (2μg) using random hexamer primers and a high-Capacity cDNA Reverse Transcription Kit (Life Technologies). Real-time qRT-PCR analysis was performed using SYBR green (Life Technologies) in 96 well plates in a 7500 FAST Applied Biosystems instrument. All reactions were run in triplicate: amplified at 95° C for 20 s, followed by 40 cycles of 95° C for 3 s and 60° C for 30s. Single peak melting curves confirmed the absence of primer-dimer complex formation. Only single bands were detected when PCR products were electrophoresed on 2% agarose gel (not shown). The primers for amplification of Cx43, GAPDH, Cx40 (total), and Cx40 transcript variant A are listed in Supplemental Table 2. For Cx40 transcript variant B mRNA, we used QuantiTect Primer Assay cat no QT01001322 (Qiagen), since these proprietary primers gave results that best satisfied our quality controls. Each experiment included samples lacking template or reverse transcriptase as negative controls.

The relative expression of each mRNA was calculated using the delta CT method and normalized to the expression of GAPDH as we have done previously [5].

### 2.8. Isolation of genomic DNA and sequence analysis of the Cx40 promoter and coding regions

Genomic DNA was isolated from left atrial appendage samples (weighing 25–40 mg) using QIAamp DNA Mini Kit (Qiagen). The average yield was 10 μg of high quality DNA. PCR was performed using Phusion High-Fidelity DNA Polymerase (Fisher Scientific) to amplify the Cx40 coding region (within exon 2) or the regions flanking Cx40 promoters A and B. PCR primers are listed in Supplemental Table 2.

To test for the single nucleotide polymorphisms (SNP) rs35594137 and rs10465885, Cx40 promoter regions A and B region were directly sequenced using the primers shown in Supplemental Table 2.

The coding region PCR products were subcloned into pCR-BluntII using the Zero Blunt® TOPO® PCR Cloning Kit (Life Technologies) and transformed into bacteria. Individual colonies (≥20 per patient) were picked and their inserts were sequenced using SP6 forward and M13 reverse primers at the DNA Sequencing Facility and Genotyping Facility of the University of Chicago.

## 3. Results

### 3.1. Cx40 levels are reduced in homogenates of atria from patients with AF

In order to determine any alterations in the atrial levels of connexins in patients with AF, we prepared homogenates from atria of control hearts and patients with paroxysmal or chronic AF and detected Cx43 or Cx40 by immunoblotting (Fig. 1). Levels of Cx43 were similar in all samples and did not differ significantly between control and AF samples (Fig. 1A). However, levels of Cx40 were reduced in atrial homogenates from patients with chronic AF and from many patients with paroxysmal AF (see exemplary blots and graphs in Fig. 1B). The mean Cx40 level was 77% of control values in the PAF samples and only 49% of controls in the CAF samples. Since Cx40 levels were much lower in all CAF samples than in controls, the mean CAF level was significantly lower than that of the controls. In contrast, Cx40 levels varied widely between PAF samples; some were very low, but others were similar to controls. *In addition, Cx40 protein levels sometimes varied between different tissue pieces from the same patient (data not shown).* Thus, the mean PAF level across all samples did not differ significantly from the control mean.

### 3.2. Cx40 is selectively lost from atrial gap junctions in patients with AF

We also studied the abundance and distribution of Cx43 and Cx40 in the atria of control hearts and several patients with paroxysmal or chronic AF. Multiple frozen sections were cut from each sample, and Cx43 and Cx40 were simultaneously detected by double label immunofluorescence. As illustrated by the examples shown in Fig. 2, both connexins were abundantly detected in discrete spots (presumably corresponding to gap junction plaques) in control atria. The two connexins co-localized extensively with only a few spots containing only Cx43 and very rare spots containing only Cx40 (as shown in the overlay image and the cytofluorogram scatter plot).

In the representative PAF and CAF sections (Fig. 2), the abundance of Cx43 appeared similar to the control section. However, the number of spots containing immunoreactive Cx40 was substantially reduced in the PAF section and severely reduced in the CAF section. *The overlap images showed that many spots in the PAF sample and an even higher proportion of gap junction plaques in the CAF sample contained Cx43, but not Cx40. The scatter plots show the shift towards a preponderance of Cx43 staining in the PAF and CAF images.*

To examine the generality of these changes, we performed similar double label immunofluorescence studies on sections from multiple control *(n = 6)*, PAF *(n = 8)*, and CAF *(n = 5)* patients. We studied the greatest number of PAF samples, because they showed the greatest variability of the extent of Cx40 staining and its overlap with Cx43. For all of the samples, we studied the overlap of Cx43 and Cx40. As described in Methods, we quantified the overlap by calculating Mander's coefficients. A Mander's coefficient of 1.0 would specify perfect overlap, while a coefficient of 0 would indicate no overlap.

We defined the variables such that Mander's coefficient M1 was a measure of the overlap of Cx43 on Cx40 (i.e., the proportion of pixels containing Cx40 that also contained Cx43). Consistent with the overlap example (Fig. 2), the mean M1 for control hearts was very high. The mean M1 for all control hearts was 0.82 (Fig. 3A). There was no significant change in the overlap of Cx43 on Cx40 detected in the diseased hearts. The mean M1 was 0.83 for both the PAF and CAF groups (Fig. 3A).

The overlap of Cx40 on Cx43 (the fraction of Cx43-containing gap junctions that also stained for Cx40) was not different among the group of control samples, since the average M2 value from the controls was 0.82 (Fig. 3B). However, M2 was significantly reduced in the PAF atria (group mean = 0.53) and significantly reduced even further in the CAF atria (group mean = 0.29) (Fig. 3B).

Individual control samples showed little variation of immunostaining for Cx43 or Cx43 between samples or among different fields in a single sample. Consistently, the range of M2 values for control hearts showed little variation from the mean (Fig. 3C). In contrast, the Cx40 abundance and co-localization showed more variability in the diseased hearts. All samples from CAF patients showed mean M2 values of < 0.5, but many had wider ranges of values than the controls (Fig. 3C). Some of the PAF samples had severe reductions of M2 while others had mean M2 values that were nearly as high as the controls. Many of the PAF samples had a wide range of M2 values calculated for different sections from the same patient (Fig. 3C). This wide range provides some quantification of the substantial heterogeneity of Cx40 (and its co-localization) within PAF patients.

The mean M2 values for the individual patients that were studied by immunofluorescence showed a relatively strong correlation with the levels of Cx40 protein detected in atrial homogenates (r = 0.78, Supplemental Fig. 1).

To determine whether remodeling of atrial gap junctions was associated with AF, we performed co-localization of the connexins vs. the intercalated disc adhesive protein, N-cadherin. As expected, Cx43 and N-cadherin showed extensive (but not perfect) overlap in

sections of control atrium (Fig. 4, left panels). The distributions of these two proteins and their overlaps were very similar in the diseased samples (representative examples shown in Fig. 4, center and right panels). We quantified the extent of overlap of Cx43 and N-cadherin in sections obtained from multiple control, PAF, and CAF patient samples (Table 1). The degree of colocalization of Cx43 and N-cadherin in our experiments was comparable to that in normal human ventricle [13]. The mean Mander's coefficients M1 (assessing the N-cadherin pixels that also contained Cx43) and M2 (assessing Cx43 pixels that also contained N-cadherin) did not differ significantly between control and diseased samples. In control tissues, Cx40 and N-cadherin showed extensive overlap similar to that between Cx43 and N-cadherin (Fig. 5, left panels). Quantitation of their overlap for the example shown in Fig. 5 yielded an M1 of 0.55 (for overlap of Cx40 on N-cadherin) and an M2 of 0.50 (for overlap of N-cadherin on Cx40). In contrast, the abundance of Cx40 was greatly reduced in the PAF and CAF samples (Fig. 5, center and right panels). As shown in these examples, the remaining Cx40 still showed substantial overlap with N-cadherin (M1, 0.62 for PAF and 0.58 for CAF examples shown). However, most N-cadherin staining showed no co-localizing Cx40 (M2, 0.04 for PAF and 0.02 for CAF examples shown). We found similar results in several different control and diseased patient samples (not shown). We conclude that the overall abundance and cellular distribution of Cx43 (relative to the intercalated discs) is preserved in the AF samples without extensive remodeling; the major change is loss of Cx40.

Because myocardial fibrosis can contribute to the pathogenesis of AF, we assessed the content of extracellular areas in sections of control and diseased atria. We performed staining with fluorescent WGA, which has similar staining properties to Masson's trichrome, used to detect collagen [12]. Images of control, PAF, and CAF atrial sections showed similar patterns and extents of staining with WGA-Texas Red-X (Supplemental Fig. 2). We found no significant difference in the percentage of tissue area that reacted with WGA between control (n = 6), PAF (n= 8), and CAF (n = 5) patient samples (Supplemental Table 3).

### 3.3. Cx40 transcripts are reduced in atrial homogenates of patients with AF

In order to determine if the alterations in connexin protein levels reflected changes in mRNA, expression, we isolated total RNA from the atria of control hearts and patients with paroxysmal or chronic AF and detected Cx43 or Cx40 mRNAs by qRT-PCR (Fig. 6A, B). The levels of Cx43 mRNA did not differ significantly between control and diseased samples (Fig. 6A). In contrast, the total levels of Cx40 mRNA (detected using primers within exon2 as described in Methods) were significantly lower in samples from patients with either PAF or CAF (Fig. 6B).

The human Cx40 gene contains two different first exons that are used alternatively to generate two different transcripts, trA and trB, after splicing with exon 2 (Fig. 6C). Therefore, we also used qRT-PCR to detect and quantify these two Cx40 transcripts. We found that both trA and trB were significantly reduced in samples from patients with PAF or CAF (Fig. 6D, E).

Moreover, although levels of total Cx40 mRNA had only a weak correlation with levels of Cx40 protein (r = 0.60) and trA showed no correlation (r = 0.30), levels of trB showed reasonably strong correlations with both levels of Cx40 protein determined by immunoblotting and the Mander's coefficient M2 (r = 0.60 and 0.77, respectively) (Supplemental Fig. 3)

### 3.4. AF patients did not carry detectable Cx40 mutations

Because germ-line and somatic mutations of Cx40 have been identified in some patients with AF [14–16], we also screened our atrial samples for such mutations. We used a rather similar strategy to that which identified the somatic mutants [14]. As described in Methods, we prepared genomic DNA from the atrial samples and amplified the entire Cx40 coding region which was subcloned into a bacterial plasmid. Even after sequencing many colonies (≥20 perpatient), we did not identify any coding region mutations in any AF patient.

### 3.5. Promoter polymorphisms may be linked to AF

The Cx40 promoters contain polymorphic variants that have been linked to AF (and other disease states including hypertension) in some studies [17–21]. We used PCR to amplify the regions flanking exons 1A and 1B (from all control and AF patient samples) and directly sequenced the DNA products to identify these polymorphisms (Supplemental Fig. 4).

The exon 1A transcriptional initiation site is flanked by two closely linked polymorphisms −44 (G→A) and +71 (A→G) (Fig. 6C) [17]. We also identified these polymorphisms in our samples (Table 1). However, we found no significant differences in frequencies of the genotypes between our control, PAF, or CAF groups. We found that 63–75% of patients in each group were homozygous for the −44G/+71A genotype and 25–37% were heterozygous for −44G/+71A and −44A/+71G. These are relatively close to the frequencies of these genotypes identified in control populations in other studies [17–20]. We did not find any individuals who were homozygous for the −44A/+71G allele which has been linked to AF in some studies [17]. We found no correlation between the genotypes at this position and the levels of Cx40 protein or mRNA in control or patient samples (data not shown).

Promoter B also contains a common polymorphism, −26; (A→G) (Fig. 6C) [19]. We found that about half of patients in all groups were heterozygous for each variant (Table 2), consistent with the expected high frequency of both alleles. We did not find any significant differences in frequencies of the different genotypes between groups. Indeed, although the −26G allele has previously been linked to AF and reduced levels of Cx40 mRNA expression, we found higher percentage of AF patients that were homozygous for the −26A allele and fewer AF patients that were homozygous for the −26G allele (Table 2). We found no correlation between the genotypes at this position and the levels of Cx40 protein or mRNA in control or patient samples (data not shown).

## 4. Discussion

In this paper, we found that there is extensive overlap of Cx40 and Cx43 immunoreactivities in normal human atrium. Nearly all of the atrial gap junctions contained both connexins. This observation is consistent with our previous demonstration (using both biochemical and

physiological approaches) that Cx40 and Cx43 make approximately equal contributions to the gap junctions between mouse atrial myocytes [5].

We have also shown that atrial tissues from patients with both chronic and paroxysmal AF contained reduced abundances of Cx40. Moreover, they exhibited reduced overlap of Cx40 immunoreactivity with Cx43, including the presence of many gap junctions that contained only Cx43. It is likely that this alteration contributes to the abnormal conduction within the atria of these hearts. A previous study found differing electrical conduction in strands of cultured neonatal murine cardiac myocytes based on genetic alterations of the relative expression of Cx40 or Cx43, such that local propagation velocity was decreased by predominance of Cx40 and increased by greater Cx43 [22]. Thus, our AF heart samples might contain areas with faster as well as slower local conduction and might vary substantially. In human atrium, the relative abundance of Cx40 as detected by immunolocalization or by immunoblotting has been correlated with reduced conduction velocity [9] and with the increased atrial resistivity associated with aging [23].

There are a number of previous studies that examined Cx40 and/or Cx43 in the atria of people or animals with AF. Previous studies that examined connexin levels by immunoblotting in atria of people with chronic AF arrived at conflicting conclusions, including increased Cx40 [24], reduced Cx40 [25], or reduced Cx43 with changes in Cx40 that varied according to biopsy site [26]. Many prior studies only looked at the distributions of Cx43 or Cx40 and Cx43 by immunohistochemistry. In a study that is particularly relevant to our own, Wilhelm et al. [10] found that the Cx40/Cx43 ratio was reduced (by ~50%) in patients with persistent or postoperative AF. Kato et al. [6] compiled the data from 12 studies using animal models and 13 studies of humans with AF of various etiologies, and while many results disagree, connexin alterations have frequently identified. A strength of our study is that we looked relatively comprehensively at multiple aspects, including protein levels, mRNA expression, and connexin distribution. Many prior studies are confounded by the presence of valvular or coronary artery disease. Some studies may also have been confounded by cellular/tissue remodeling or fibrosis that were not present in our patients.

When we analyzed the samples from patients with paroxysmal AF, we found a substantial variability both within samples and between samples (especially in the Cx40/Cx43 ratio as quantified by the Mander’s coefficient, M2). Some patients had coefficients similar to the normal controls, while others were less than half as great; moreover, a single sample ranged from 0.0 to >0.6 (Fig. 3C). These findings emphasize the pronounced heterogeneity of connexin distribution in these patients with intermittent AF. Our findings recall goat studies in which the distribution of Cx40 was homogeneous for animals in sinus rhythm, but it became markedly heterogeneous after 2 weeks of AF [27, 28]. Like that study, our data support the hypothesis that changes in Cx40 distribution are involved in the electrical remodeling that contributes to the pathogenesis of sustained AF.

Both somatic and germ-line mutations of Cx40 have been identified in patients with lone AF [14–16, 29]. These mutations apparently contribute to AF by reducing the abundance of functional Cx40. Responsible mechanisms can include alterations or loss of channel function [14, 16, 30], impaired Cx40 trafficking [30], or increased Cx40 degradation [31].

However, like another study of a group of these patients [32], we did not find any evidence for coding region mutations in our patients. Some previously identified patients may have been unique because of their relatively young ages (onset of AF at an average age of 45 in the study by Gollob et al. [14]). Regardless, it is apparent that coding region mutations of Cx40 are an uncommon pathogenic cause of AF.

Our conclusions regarding the importance of Cx40 disturbances in the etiology of human AF are supported by some investigations of genetically manipulated mice. Some studies of Cx40 null mice, mice with Cx45 replacement of Cx40, and mice carrying the Cx46A96S mutation showed decreased atrial conduction velocities [33–36]. Indeed, pacing can induce atrial tachyarrhythmias or fibrillation in Cx40-null mice [33, 37, 38]. However, unlike the heterogeneity of Cx40 loss seen in our samples, the global genetic disruptions of Cx40 expression cause uniform reductions (or absence) of atrial myocyte Cx40 in these mice [36].

The decreased Cx40 protein levels that we observed in association with AF did correlate with decreased levels of Cx40 mRNA, and in particular one Cx40 transcript, trB. Prior studies have linked AF to polymorphic variants (SNPs) of each of the Cx40 promoters [17, 19, 39]. These SNPs can cause decreased transcription of the corresponding transcripts and/or reduced Cx40 levels [19, 21]. The prior studies disagree about which SNP is linked to AF, perhaps due to the analysis of different populations. Because we found reduced Cx40 expression, but no correlation with either SNP, it is likely that the decrease in Cx40 transcription was not the primary pathogenic event.

## Conclusion

In summary, our study adds evidence supporting the importance of Cx40 alterations (especially reductions relative to Cx43) in AF. As discussed above and reviewed elsewhere [6, 40], there are many conflicting results regarding the precise changes of connexins in AF. Taking them all together, we suggest that the alterations are multifactorial and may eventually be best addressed by personalized approaches to treatment.

## Supplementary Material

Refer to Web version on PubMed Central for supplementary material.

## Acknowledgments

This work was supported by grants from the National Institutes of Health: HL59199 (to ECB), HL113640 (to XA), and UL1TR000430 (pilot funding to ECB). KBB was supported by a fellowship from the Ted Mullin fund. The authors would like to acknowledge the assistance of Zachary Bulwa in isolation of genomic DNA and sequence analysis of Cx40 promoter A and coding region.

## Abbreviations

| | |
|---|---|
| **AF** | Atrial fibrillation |
| **CAF** | chronic AF |
| **PAF** | paroxysmal AF |

| | |
|---|---|
| **Cx43** | Connexin43 |
| **Cx40** | Connexin40 |
| **SDS-PAGE** | Sodium Dodecyl Sulfate Polyacrylamide Gel Electrophoresis |
| **DIC** | differential interference contrast |
| **SNP** | single nucleotide polymorphism |
| **PCR** | polymerase chain reaction |
| **qRT-PCR** | quantitative Reverse Transcription-PCR |
| **trA and trB** | Cx40 mRNA transcripts A and B |
| **GAPDH** | glyceraldehyde phosphate dehydrogenase |
| **WGA** | Wheat Germ Agglutinin |

## Reference List


1. Allessie MA, Boyden PA, Camm AJ, kleber AG, Lab MJ, Legato MJ, et al. Pathophysiology and prevention of atrial fibrillation. Circulation. 2001; 103:769–77. [PubMed: 11156892]
2. Iwasaki YK, Nishida K, Kato T, Nattel S. Atrial fibrillation pathophysiology: implications for management. Circulation. 2011; 124:2264–74. [PubMed: 22083148]
3. Spach MS, Starmer CF. Altering the topology of gap junctions: a major therapeutic target for atrial fibrillation. Cardiovasc Res. 1995; 30:337–44. [PubMed: 7585823]
4. Saffitz JE, Kanter HL, Green KG, Tolley TK, Beyer EC. Tissue-specific determinants of anisotropic conduction velocity in canine atrial and ventricular myocardium. Circ Res. 1994; 74:1065–70. [PubMed: 8187276]
5. Lin X, Gemel J, Glass A, Zemlin CW, Beyer EC, Veenstra RD. Connexin40 and connexin43 determine gating properties of atrial gap junction channels. J Mol Cell Cardiol. 2010; 48:238–45. [PubMed: 19486903]
6. Kato T, Iwasaki YK, Nattel S. Connexins and atrial fibrillation: filling in the gaps. Circulation. 2012; 125:203–6. [PubMed: 22158757]
7. Bradford MM. A rapid and sensitive method for the quantitation of microgram quantities of protein using the principle of protein-dye binding. Anal Biochem. 1976; 72:248–54. [PubMed: 942051]
8. Bolte S, Cordelieres FP. A guided tour into subcellular colocalization analysis in light microscopy. J Microsc. 2006; 224:213–32. [PubMed: 17210054]
9. Kanagaratnam P, Rothery S, Patel P, Severs NJ, Peters NS. Relative expression of immunolocalized connexins 40 and 43 correlates with human atrial conduction properties. J Am Coll Cardiol. 2002; 39:116–23. [PubMed: 11755296]
10. Wilhelm M, Kirste W, Kuly S, Amann K, Neuhuber W, Weyand M, et al. Atrial distribution of connexin 40 and 43 in patients with intermittent, persistent, and postoperative atrial fibrillation. Heart Lung Circ. 2006; 15:30–7. [PubMed: 16473788]
11. Dolber PC, Beyer EC, Junker JL, Spach MS. Distribution of gap junctions in dog and rat ventricle studied with a double-label technique. J Mol Cell Cardiol. 1992; 24:1443–57. [PubMed: 1338112]
12. Pandya K, Kim HS, Smithies O. Fibrosis, not cell size, delineates beta-myosin heavy chain reexpression during cardiac hypertrophy and normal aging in vivo. Proc Natl Acad Sci U S A. 2006; 103:16864–9. [PubMed: 17068123]
13. Glukhov AV, Fedorov VV, Kalish PW, Ravikumar VK, Lou Q, Janks D, et al. Conduction remodeling in human end-stage nonischemic left ventricular cardiomyopathy. Circulation. 2012; 125:1835–47. [PubMed: 22412072]

14. Gollob MH, Jones DL, Krahn AD, Danis L, Gong XQ, Shao Q, et al. Somatic mutations in the connexin 40 gene (*GJA5*) in atrial fibrillation. N Engl J Med. 2006; 354:2677–88. [PubMed: 16790700]
15. Yang Y-Q, Liu X, Zhang XL, Wang XH, Tan HW, Shi HF, et al. Novel connexin40 missense mutations in patients with familial atrial fibrillation. Europace. 2010; 12:1421–7. [PubMed: 20650941]
16. Sun Y, Yang YQ, Gong XQ, Wang XH, Li RG, Tan HW, et al. Novel germline *GJA5*/connexin40 mutations associated with lone atrial fibrillation impair gap junctional intercellular communication. Hum Mutat. 2013; 34:603–9. [PubMed: 23348765]
17. Firouzi M, Ramanna H, Kok B, Jongsma HJ, Koeleman BP, Doevendans PA, et al. Association of human connexin40 gene polymorphisms with atrial vulnerability as a risk factor for idiopathic atrial fibrillation. Circ Res. 2004; 95:e29–e33. [PubMed: 15297374]
18. Firouzi M, Kok B, Spiering W, Busjahn A, Bezzina CR, Ruijter JM, et al. Polymorphisms in human connexin40 gene promoter are associated with increased risk of hypertension in men. J Hypertens. 2006; 24:325–30. [PubMed: 16508580]
19. Wirka RC, Gore S, Van Wagoner DR, Arking DE, Lubitz SA, Lunetta KL, et al. A common connexin-40 gene promoter variant affects connexin-40 expression in human atria and is associated with atrial fibrillation. Circ Arrhythm Electrophysiol. 2011; 4:87–93. [PubMed: 21076161]
20. Pfenniger A, van der Laan SW, Foglia B, Dunoyer-Geindre S, Haefliger JA, Winnik S, et al. Lack of association between connexin40 polymorphisms and coronary artery disease. Atherosclerosis. 2012; 222:148–53. [PubMed: 22405441]
21. Chaldoupi SM, Hubens LE, Smit Duijzentkunst DA, van SL, Bierhuizen MF, van Aarnhem EE, et al. Reduced connexin40 protein expression in the right atrial appendage of patients bearing the minor connexin40 allele (−44 G --> A). Europace. 2012; 14:1199–205. [PubMed: 22423256]
22. Beauchamp P, Yamada KA, Baertschi AJ, Green K, Kanter EM, Saffitz JE, et al. Relative contributions of connexins 40 and 43 to atrial impulse propagation in synthetic strands of neonatal and fetal murine cardiomyocytes. Circ Res. 2006; 99:1216–24. [PubMed: 17053190]
23. Dhillon PS, Chowdhury RA, Patel PM, Jabr R, Momin AU, Vecht J, et al. The relationship between connexin expression and gap junction resistivity in human atrial myocardium. Circ Arrhythm Electrophysiol. 2014; 7:321–9. [PubMed: 24610741]
24. Polontchouk L, Haefliger JA, Ebelt B, Schaefer T, Stuhlmann D, Mehlhorn U, et al. Effects of chronic atrial fibrillation on gap junction distribution in human and rat atria. J Am Coll Cardiol. 2001; 38:883–91. [PubMed: 11527649]
25. Nao T, Ohkusa T, Hisamatsu Y, Inoue N, Matsumoto T, Yamada J, et al. Comparison of expression of connexin in right atrial myocardium in patients with chronic atrial fibrillation versus those in sinus rhythm. Am J Cardiol. 2003; 91:678–83. [PubMed: 12633797]
26. Kostin S, Klein G, Szalay Z, Hein S, Bauer EP, Schaper J. Structural correlate of atrial fibrillation in human patients. Cardiovasc Res. 2002; 54:361–79. [PubMed: 12062341]
27. van der Velden HM, van KM, Wijffels MC, van ZM, Groenewegen WA, Allessie MA, et al. Altered pattern of connexin40 distribution in persistent atrial fibrillation in the goat. J Cardiovasc Electrophysiol. 1998; 9:596–607. [PubMed: 9654224]
28. van der Velden HM, Ausma J, Rook MB, Hellemons AJ, van Veen TA, Allessie MA, et al. Gap junctional remodeling in relation to stabilization of atrial fibrillation in the goat. Cardiovasc Res. 2000; 46:476–86. [PubMed: 10912458]
29. Shi HF, Yang JF, Wang Q, Li RG, Xu YJ, Qu XK, et al. Prevalence and spectrum of GJA5 mutations associated with lone atrial fibrillation. Mol Med Rep. 2013; 7:767–74. [PubMed: 23292621]
30. Patel D, Gemel J, Xu Q, Simon AR, Lin X, Matiukas A, et al. Atrial fibrillation-associated Connexin40 mutants make hemichannels and synergistically form gap junction channels with novel properties. FEBS Lett. 2014; 588:1458–64. [PubMed: 24457199]
31. Gemel J, Simon AR, Patel D, Xu Q, Matiukas A, Veenstra RD, et al. Degradation of a connexin40 mutant linked to atrial fibrillation is accelerated. J Mol Cell Cardiol. 2014; 74:330–9. [PubMed: 24973497]

32. Tchou GD, Wirka RC, Van Wagoner DR, Barnard J, Chung MK, Smith JD. Low prevalence of connexin-40 gene variants in atrial tissues and blood from atrial fibrillation subjects. BMC Med Genet. 2012; 13:102. [PubMed: 23134779]
33. Verheule S, van Batenburg CA, Coenjaerts FE, Kirchhoff S, Willecke K, Jongsma HJ. Cardiac conduction abnormalities in mice lacking the gap junction protein connexin40. J Cardiovasc Electrophysiol. 1999; 10:1380–9. [PubMed: 10515563]
34. Bagwe S, Berenfeld O, Vaidya D, Morley GE, Jalife J. Altered right atrial excitation and propagation in connexin40 knockout mice. Circulation. 2005; 112:2245–53. [PubMed: 16203917]
35. Alcolea S, Jarry-Guichard T, de Bakker J, Gonzalez D, Lamers W, Coppen S, et al. Replacement of connexin40 by connexin45 in the mouse: impact on cardiac electrical conduction. Circ Res. 2004; 94:100–9. [PubMed: 14630724]
36. Lubkemeier I, Andrie R, Lickfett L, Bosen F, Stockigt F, Dobrowolski R, et al. The Connexin40A96S mutation from a patient with atrial fibrillation causes decreased atrial conduction velocities and sustained episodes of induced atrial fibrillation in mice. J Mol Cell Cardiol. 2013; 65C:19–32. [PubMed: 24060583]
37. Hagendorff A, Schumacher B, Kirchhoff S, Luderitz B, Willecke K. Conduction disturbances and increased atrial vulnerability in Connexin40-deficient mice analyzed by transesophageal stimulation. Circulation. 1999; 99:1508–15. [PubMed: 10086977]
38. Bevilacqua LM, Simon AM, Maguire CT, Gehrmann J, Wakimoto H, Paul DL, et al. A targeted disruption in Connexin40 leads to distinct atrioventricular conduction defects. J Interv Card Electrophysiol. 2000; 4:459–567. [PubMed: 11046183]
39. Christophersen IE, Holmegard HN, Jabbari J, Sajadieh A, Haunso S, Tveit A, et al. Rare variants in GJA5 are associated with early-onset lone atrial fibrillation. Can J Cardiol. 2013; 29:111–6. [PubMed: 23040431]
40. Chaldoupi SM, Loh P, Hauer RN, de Bakker JM, van Rijen HV. The role of connexin40 in atrial fibrillation. Cardiovasc Res. 2009; 84:15–23. [PubMed: 19535379]

## Highlights

- Normal atrial conduction requires similar abundances of connexins (Cx40 and Cx43).
- Immunoreactive Cx40 but not Cx43 was reduced in atrial fibrillation (AF) patients.
- Reductions of Cx40 were heterogeneous (especially in paroxysmal AF samples).
- Total Cx40 mRNA and Cx40 transcripts A and B were reduced in paroxysmal and chronic AF.
- Changes of Cx40 expression did not correlate with promoter polymorphisms.

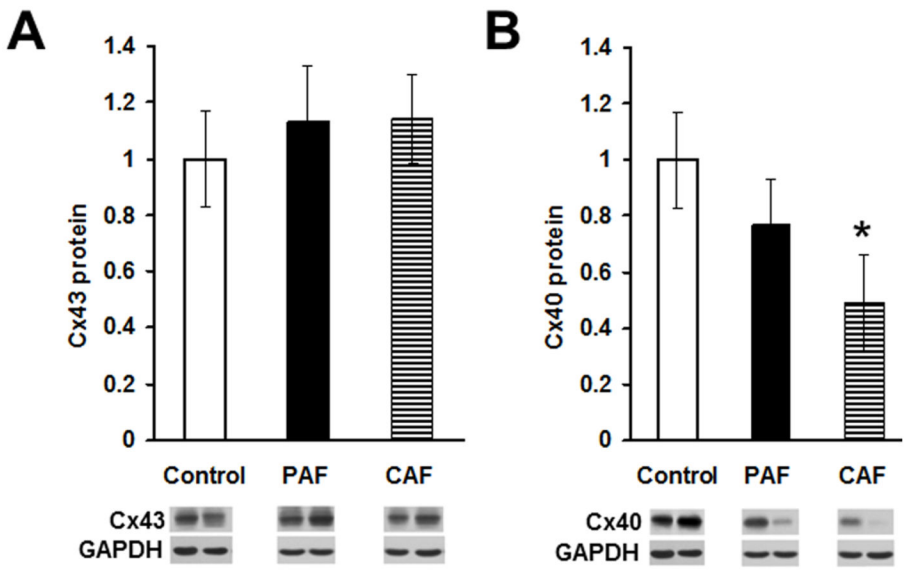


**Figure 1. Levels of Cx40 (but not Cx43) are reduced in atrial homogenates of patients with atrial fibrillation**

Homogenates were prepared from atrial appendage samples from control hearts or from patients with paroxysmal (PAF) or chronic (CAF) atrial fibrillation, and Cx43 (A) and Cx40 (B) were detected by immunoblotting. Bands at the bottom are representative blots from two control samples and from two patients with PAF or CAF. Gels were loaded with equal amounts of total protein and were also blotted with antibodies directed against GAPDH (as a loading control). Graphs show the amounts (mean ± SEM) of immunoreactive connexin in each group determined by densitometry (adjusted for GAPDH densitometry and normalized to the mean control values). While the abundance of Cx43 did not differ significantly between control and disease groups, the mean level of Cx40 in the CAF group (but not the PAF group) was significantly less than in controls *(*, $p < 0.05$, Student's t test)*.

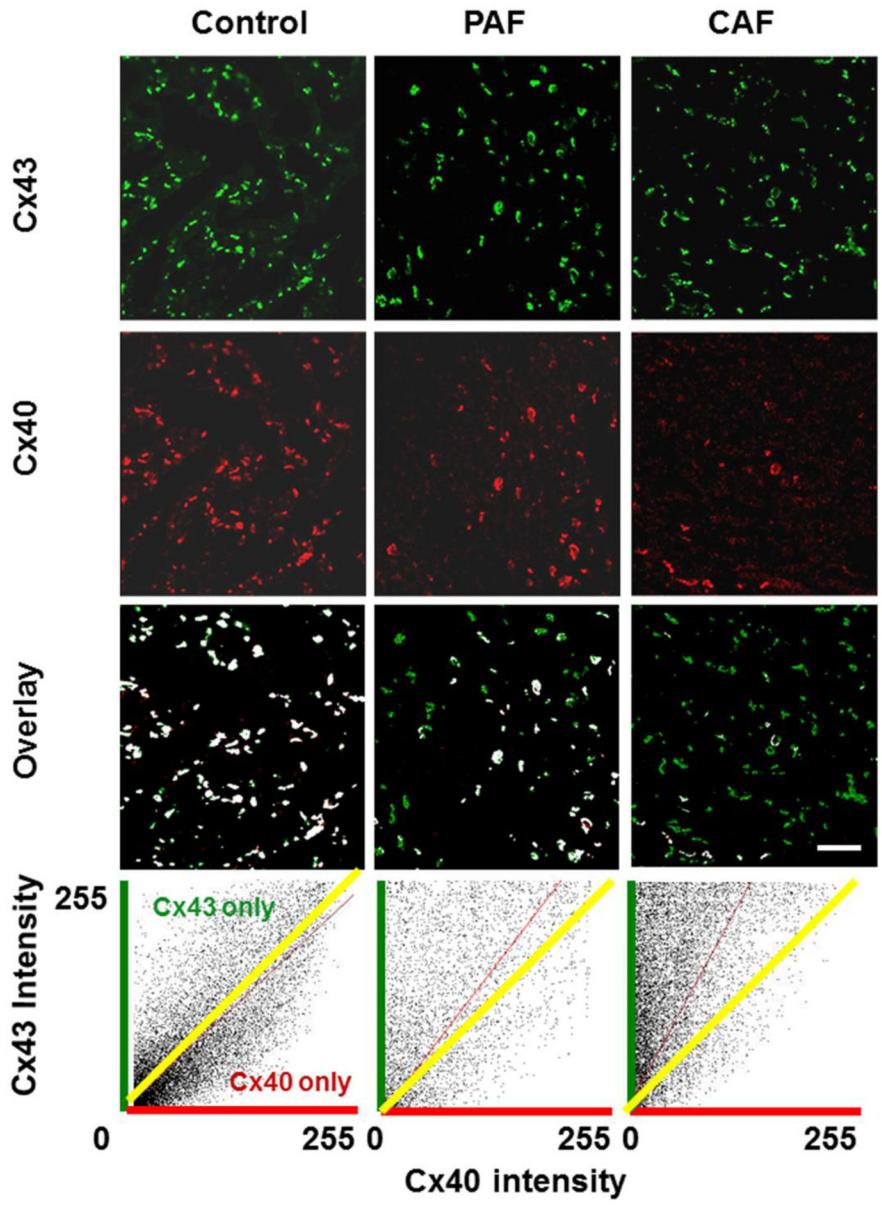


**Figure 2. Immunolocalization of Cx43 and Cx40 shows reductions of Cx40 in sections from hearts of patients with atrial fibrillation**

Representative photomicrographs are shown for sections from atrial appendage samples from control hearts (left panels) or from patients with paroxysmal (PAF, center panels) or chronic (CAF, right panels) atrial fibrillation that were studied by double label immunofluorescence for Cx43 (green, top row) and Cx40 (red, second row). The third row shows the overlay between Cx43 and Cx40; spots containing both connexins are shown in white, while those containing only Cx43 are green and those containing only Cx40 are red. While the abundance of Cx43 appears similar in all three samples, Cx40 is diminished in PAF and severely reduced in CAF. This results in fewer white spots and many “green only” spots in the overlay images for PAF and CAF. The bottom panels show cytofluorogram scatter plots of the intensities of all pixels; Cx43 and Cx40 intensities are quantified

according to a 0 – 255 gray scale. The yellow line shows the theoretical predicted mean for a perfect overlap of the distribution and intensities of Cx40 and Cx43. The red lines show the determined distributions, and illustrate the shift towards Cx43 predominance in the atrial fibrillation samples and the selective loss of Cx40. Bar, 42 μm.

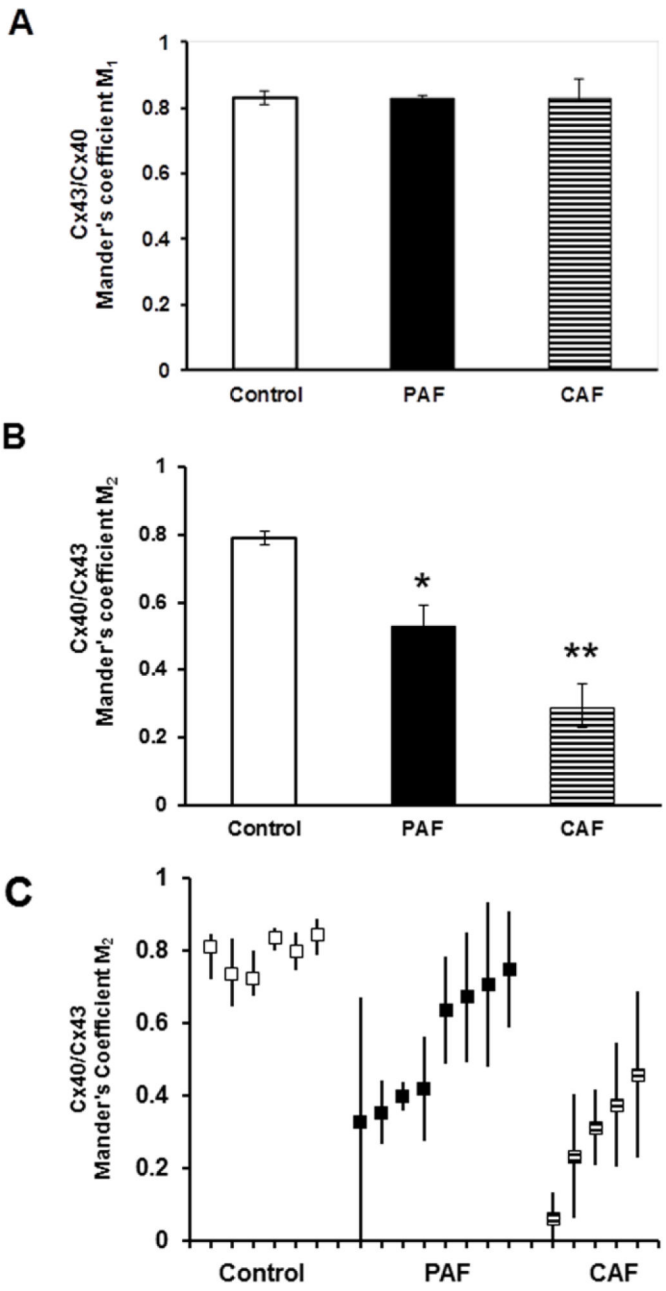


**Figure 3. Co-localization coefficients show that Cx40 was reduced relative to Cx43 in atria of patients with atrial fibrillation**

The distribution of Cx43 and Cx40 and their overlap were determined by immunofluorescence (as illustrated in Fig. 2) for multiple sections from each control and diseased sample. For each section the overlap was quantified by calculating the Mander's coefficients as described in Methods. A coefficient of 1.0 indicates perfect overlap while a coefficient of 0 indicates no overlap. Variables were defined so that Mander's coefficient M1 is an expression of the overlap of Cx40 on Cx43 (Cx40 spots that also contain Cx43) and Mander's coefficient M2 is an expression of the overlap of Cx43 on Cx40 (Cx43 spots that also contain Cx40). (**A. B**) The graphs show the Mander's M1 (A) and M2 (B)

coefficients (mean ± SEM) for groups of control (n = 6), PAF (n = 8), and CAF (n = 5) samples. Mean M1 values did not show any differences between control and diseased specimens. However, mean M2 values were reduced in PAF samples as compared to controls *(*, $p < 0.05$, ANOVA)* and reduced in CAF samples as compared to either controls or PAF samples *(**, $p < 0.05$, ANOVA)*. These data quantify the selective loss of Cx40 from gap junctions in the atria of patients with paroxysmal and chronic atrial fibrillation. (**C**) The graph shows the mean M2 coefficient (solid squares) for each control, PAF or CAF sample analyzed. The bars represent the range of different M2 values determined from images of different sections in the same individual. Thus, there was a wide variation between AF patients (especially those with PAF) and within many individual AF patients.

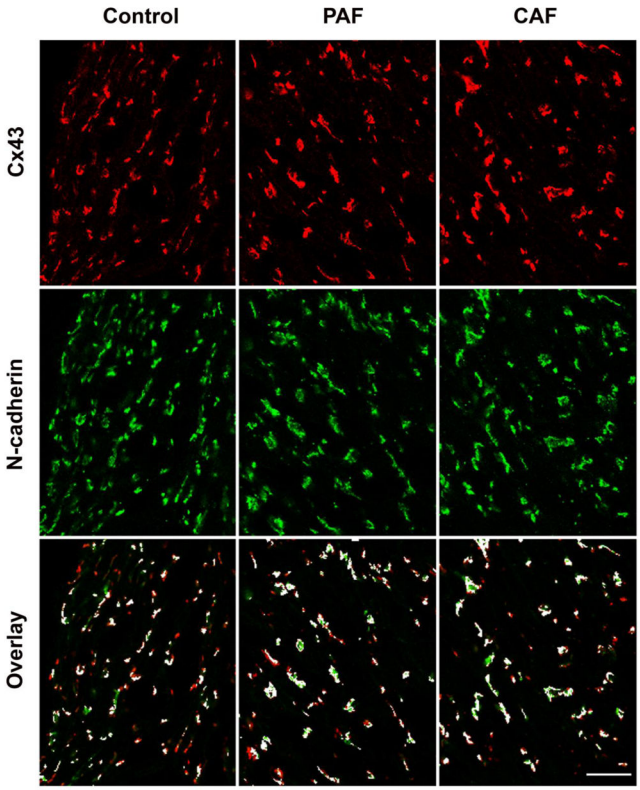


**Figure 4. Immunolocalization of Cx43 vs. N-cadherin does not differ between control and AF patients**

Representative photomicrographs are shown for sections from atrial appendage samples from control hearts (left panels) or from patients with paroxysmal (PAF, center panels) or chronic (CAF, right panels) atrial fibrillation that were studied by double label immunofluorescence for Cx43 (red, top row) and N-cadherin (green, second row). The third row shows the overlay between Cx43 and N-cadherin; spots containing both proteins are shown in white, while those containing only Cx43 are red and those containing only N-cadherin are green. The abundance of Cx43 and N-cadherin appears similar in all three samples. Bar, 40 μm.

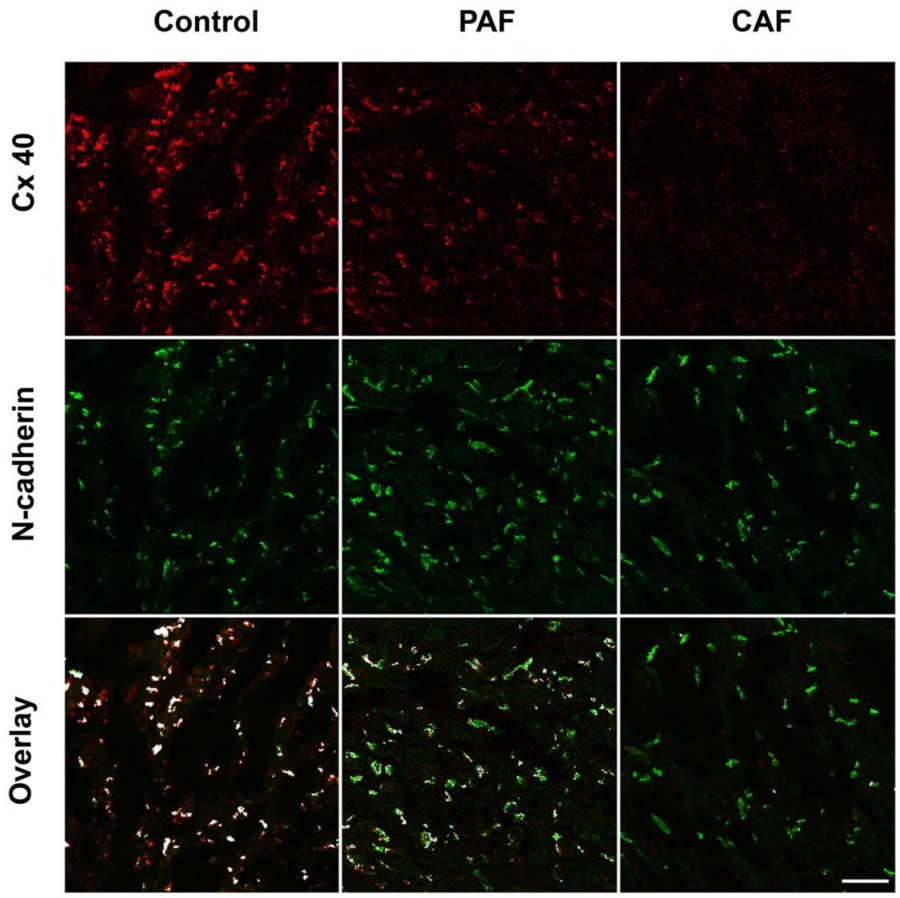


**Figure 5. Immunolocalization of Cx40 and N-cadherin shows reductions of Cx40 in sections from hearts of patients with atrial fibrillation**

Representative photomicrographs are shown for sections of atrial appendage samples from control hearts (left panels) or from patients with paroxysmal (PAF, center panels) or chronic (CAF, right panels) atrial fibrillation that were studied by double label immunofluorescence for Cx40 (red, top row) and N-cadherin (green, second row). The third row shows the overlay between Cx40 and N-cadherin; spots containing both connexins are shown in white, while those containing only N-cadherin are green and those containing only Cx40 are red. While the abundance of N-cadherin appears similar in all three samples, Cx40 is diminished in PAF and CAF. This results in fewer white spots and many “green only” spots in the overlay images for PAF and CAF. Bar, 40 μm.

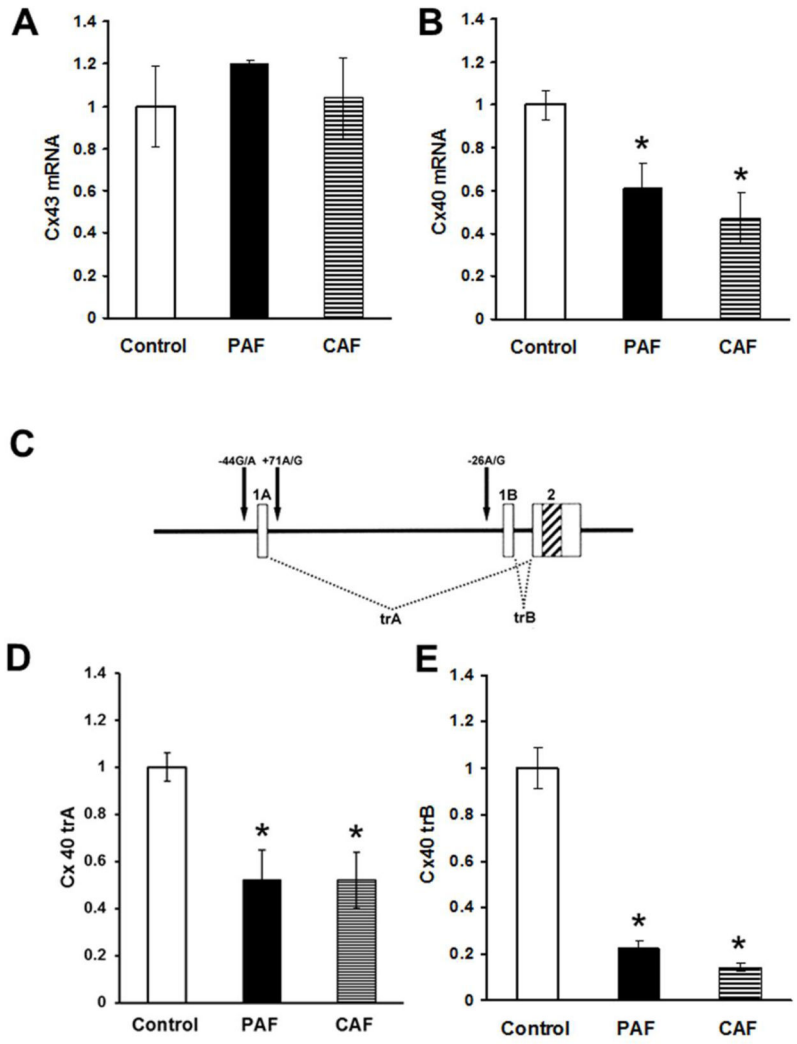


**Figure 6. Levels of Cx40 (but not Cx43) mRNA are reduced in atrial homogenates of patients with atrial fibrillation**

Total RNA was prepared from atrial homogenates of control hearts or patients with paroxysmal (PAF) or chronic (CAF) atrial fibrillation. Total mRNAs for Cx43 (A) and Cx40 (B) were quantified by qRT-PCR. Graphs show the values normalized to the average values in control samples (mean ± SEM). (A) Total levels of Cx43 mRNA did not differ among groups. (B) Total levels of Cx40 mRNA were significantly reduced in both PAF and CAF groups. (C) A diagram illustrates the structure of the Cx40 gene and the mRNAs generated from it. The gene contains two alternate first exons (1A and 1B) a single second exon (2) indicated by boxes with the coding region indicated by diagonal stripes. Differential exon usage leads to the production of two different transcripts (trA and trB). The two transcriptional start sites are flanked by polymorphic variants (−44G/A and +71A/G for A and −26A/G for B) that are indicated by arrows. (D, E) Levels of both Cx40 trA (panel D) and trB (panel E) were significantly reduced in both PAF and CAF groups *(*, $p < 0.05$ as compared to controls)*.

## Table 1

Mander's coefficients assessing co-localization of Cx43 and N-cadherin.

| | M1 (Cx43 on N-cadherin) | M2 (N-cadherin on Cx43) |
|---|---|---|
| Control (5) | 0.69 ± 0.05 | 0.56 ± 0.03 |
| PAF (8) | 0.68 ± 0.03 | 0.58 ± 0.02 |
| CAF (5) | 0.73 ± 0.02 | 0.60 ± 0.06 |

Numbers of different patient samples analyzed are indicated in parentheses. At least 5 fields were analyzed for each sample. Values are shown as mean ± S.E.M. Mean M1 and M2 values did not show any significant differences between control and diseased specimens.

## Table 2

Frequencies of Cx40 promoter polymorphic genotypes.

| | Promoter A Genotype | | |
|---|---|---|---|
| | **−44GG/+71AA** | **−44GA/+71AG** | **−44AA/+71GG** |
| Control | 75% (6/8) | 25% (2/8) | 0 |
| PAF | 69% (11/16) | 31% (5/16) | 0 |
| CAF | 63% (5/8) | 37% (3/8) | 0 |

| | Promoter B Genotype | | |
|---|---|---|---|
| | **−26AA** | **−26AG** | **−26GG** |
| Control | 13% (1/8) | 50% (4/8) | 37% (3/8) |
| PAF | 31% (5/16) | 44% (7/16) | 26% (4/16) |
| CAF | 25% (2/8) | 62% (5/8) | 13% (1/8) |

Genotype frequencies are shown as percentages with n/total number per group indicated in parentheses. The chi-squared test was used to compare groups. None of the disease groups differed from controls.